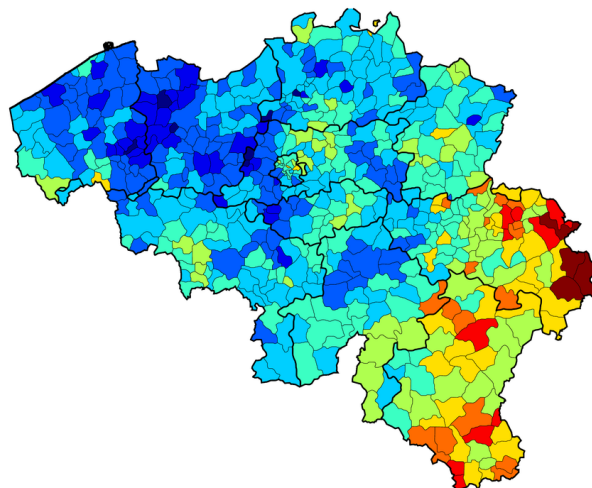


Koninklijk Meteorologisch Instituut van België
Institut Royal Météorologique de Belgique
Royal Meteorological Institute of Belgium



A cloud-to-ground lightning climatology for Belgium



Dieter R. Poelman, Laurent Delobbe

2015

Wetenschappelijke en
technische publicatie
N^o 66

Uitgegeven door het
**KONINKLIJK METEOROLOGISCH
INSTITUUT VAN BELGIE**
Ringlaan 3, B-1180 Brussel
Verantwoordelijke uitgever: Dr. D. Gellens

Publication scientifique
et technique
N^o 66

Edité par
**L'INSTITUT ROYAL METEOROLOGIQUE
DE BELGIQUE**
Avenue Circulaire 3, B-1180 Bruxelles
Editeur responsable: Dr. D. Gellens

A cloud-to-ground lightning climatology for Belgium
Dieter R. Poelman and Laurent Delobbe

Scientific committee:

Prof. dr. Ir. Christian Bouquegneau, dr. Maarten Reyniers,
dr. Christian Tricot, Luc Debontridder, dr. Michel Journée

Contents

Abstract	1
1 Introduction	1
2 Data	2
3 Methodology	4
4 Results and analysis	4
4.1 Temporal statistics	4
4.2 Spatial statistics	5
4.3 Presenting the data to the end-user	10
4.3.1 Smoothing	11
4.3.2 Lightning density at municipal and provincial level	11
5 Summary	13
References	15

Abstract

In this study, spatial and temporal characteristics of cloud-to-ground (CG) lightning in Belgium are presented. For this, observations made by the EUCLID network spanning a period of 10 years between 2004 and 2013 are collected and analyzed.

It is found that mean CG flash densities vary between $0.3 \text{ km}^{-2}\text{yr}^{-1}$ in the west up to $1.8 \text{ km}^{-2}\text{yr}^{-1}$ toward the east of Belgium, based on a spatial resolution of $5 \times 5 \text{ km}^2$. The average flash density in Belgium is $0.7 \text{ km}^{-2}\text{yr}^{-1}$. The same behavior is found in terms of thunderstorm days and hours, where in the east more activity is observed with a drop-off toward the coast. The majority of lightning activity takes place in the summer months between May and August, accounting for nearly 90% of the total activity. Furthermore, the thunderstorm season reaches its highest activity in June-July in terms of CG detections, while the diurnal cycle peaks between 1500 and 1600 UTC.

In addition, there is a growing need to present the data in a clear and concise way. This should be tailored to the needs of the enquirer, but is also limited to what is technically possible. This is certainly true when displaying for instance the CG flash density N_g . A different approach is required since the level of details needed depends strongly on the target group. Obviously, to evaluate the risk of lightning damage for a specific building or storage facility, a higher level of detail is required in order to put an adequate protection in place, than when, for example, general info is requested by the media. Therefore, great attention is given to the different possibilities to present the flash density in Belgium. We propose that, besides displaying N_g graphically as a function of an underlying spatial resolution, it can be more sensible in some cases to allocate one value per commune or province when a detailed distribution of the flash density is not desired.

1 Introduction

Electrification has always grasped the interest and fascination of people. Over decades now, continuous efforts have further improved our understanding of this natural phenomenon. Present-day advancements are driven by the possibility to tackle unsolved questions from different angles. The outcome is not only relevant from a pure scientific point of view, but is considered to be of great value as well for engineers wanting to protect electronic systems from the deleterious effects of lightning. This is certainly true for the ground flash density N_g , defined as the number of CG lightning flashes per km^2 per year, since this parameter plays a vital role in the risk analysis.

Lightning discharges are a combination of complex physical processes, radiating throughout the full spectrum domain of electromagnetic fields, from the very low frequencies (VLF) up to the very high frequencies (VHF) and into the optical. Even X-ray emission has been frequently detected in association with rocket-triggered lightning (Dwyer et al. 2011). As such, different detection and localization techniques are best suited to handle particular radiation patterns linked to a certain process in the formation of a lightning discharge. In the remainder of this publication focus is on the observed CG lightning characteristics in Belgium. Hence, a brief description of some of the different stages in the formation of a CG discharge is here at place. A typical thundercloud consists of areas of opposite charge, i.e., negative versus positive, as a consequence of complex interactions of different (icy) particles within the cloud. As such, strong electric fields are present which can lead to an electric discharge to ground. This discharge is a collection of electrons that move from cloud to ground in rapid luminous steps, hence the name “stepped leader”. When this stepped-leader approaches ground, the electric field between ground and the stepped-leader is locally enhanced, so much so that an

upward-moving discharge from ground is launched. The moment that the stepped leader and the upward moving discharge connect, a return stroke (RS) is initiated, and is nothing more than the movement of large amounts of electrons toward ground. The emitted radiation in LF, around 10 kHz, characterizes this return stroke (RS) of a CG lightning discharge. After this RS, the whole process can stop or continue, producing more strokes toward ground. Hence, a CG flash, being the combination of one or multiple CG strokes, can consist out of one or multiple CG strokes. In case of the latter, a particular stroke is assigned to an existing flash only when it follows specific spatial and time criteria, as described in more detail in Sect. 3.

In the past, when technology was not as advanced as present-day lightning locations systems (LLS), N_g at a particular location was extracted based on the amount of observed thunderstorm days T_d by a human observer. In this way, a thunderstorm day is defined as an observational day (any 24-hour period selected as the basis for climatological or hydrological observations) during which thunder is heard. Note that the requirement that thunder should actually be heard limits the area covered by each observing point. Various relationships have been published ever since (Prentice, 1977) correlating N_g and T_d depending on, e.g., geographical regions, and are mostly of the following form:

$$N_g = aT_d^b \quad [\text{km}^{-2}\text{yr}^{-1}], \quad (1)$$

with a and b variables. Nevertheless, not two thunderstorms are identical and produce the same amount of lightning. Hence, the above N_g - T_d relation can only provide an initial guess about the true amount of occurred CG flashes.

Even though over the last few decades the technology used by LLS became more and more advanced, it remains challenging to determine the true geographical distribution of CG lightning flashes. Even in the case that distinct LLS observe lightning pulses in the same frequency range, the outcome may differ due to a difference in network geometry, thresholds used, processing algorithms and the fact that the networks will unlikely have similar detection efficiencies (Poelman et al. 2013a). To account for the latter and for the variable nature of lightning incidence from year to year, reliable insights into the lightning activity in Belgium can only be achieved when based on large amounts of data. Hence, a sufficiently long sampling period is required to ensure that short time variations do not affect statistics.

In the following, a total of 215 000 CG flashes recorded between 2004 and 2013 are used to analyse the spatial and temporal characteristics of the CG electrical activity in Belgium. The lightning data used throughout this study are described in Sect. 2. Treatment of the data to produce the temporal and spatial maps is included in Sect. 3. Sect. 4 is reserved to illustrate and interpret the results, while Sect. 5 concludes with a summary.

2 Data

From 2001 onward several national meteorological services (NMS) and commercial companies within Europe joined forces to combine their respective operational LLS into the so-called European Cooperation for Lightning Detection (EUCLID). This is possible since all the individual sensors within the EUCLID network operate over the same LF spectrum range. As such, the individual raw sensor data are sent in real time to a single central processor, calculating the electrical activity at any given moment. The use of a common central processor ensures that the resulting data are as consistent as possible throughout Europe, and is frequently of higher quality opposed to a simple composite of the individual LLS due to the implicit redundancy produced by shared sensor information. The location of EUCLID sensors in the neighbourhood of Belgium are depicted in Fig. 1, with one sensor positioned at Ernage, Belgium. More informa-

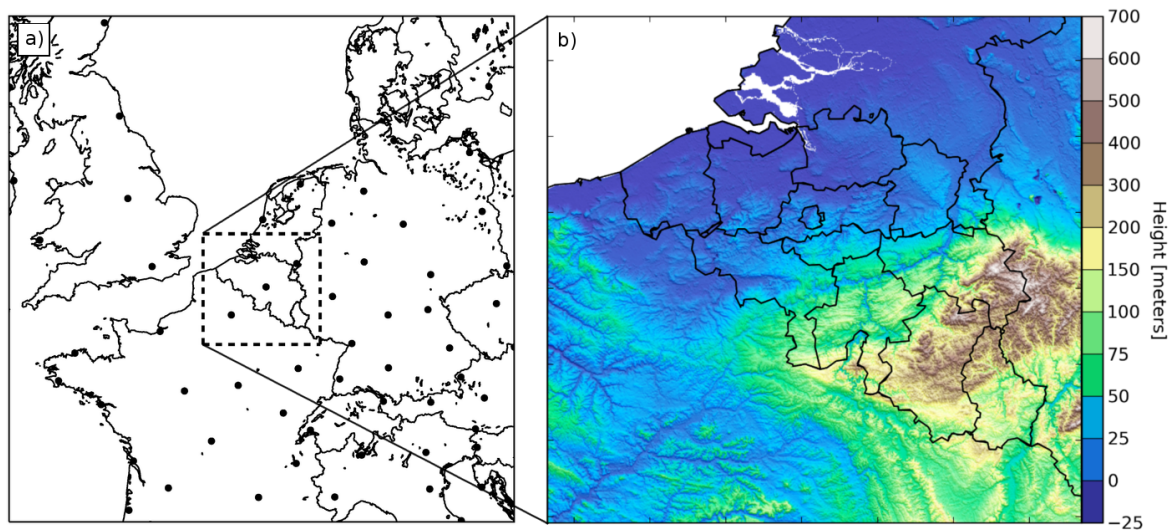


Figure 1: a) Location of some of the EUCLID sensors (dots) in and around Belgium and b) the topography of Belgium.

tion about the setup of EUCLID can be found in Schulz and Diendorfer (2002) and Diendorfer (2002).

The performance of EUCLID has been frequently tested over the years in terms of its location accuracy (LA), detection efficiency (DE), and peak current estimation, made possible by comparing to direct lightning measurements at the Gaisberg tower (GBT) in Austria (Diendorfer et al. 2011) and/or to data obtained by a mobile video and electric field recording system (VFRS) taken at different locations (Schulz et al. 2014). Most recent validation efforts employing the VFRS took place at various locations in Austria from 2009 and 2012 (Schulz et al. 2012), in Belgium throughout August 2011 (Poelman et al. 2013b), and during the Hydrological Cycle in Mediterranean Experiment (HYMEX) in southern France (Ducrocq et al. 2013) in 2012. Based on the ground truth campaign in Belgium, most relevant for this study, the median relative LA is 600 m, whereas the DE for negative strokes and flashes reaches 84% and 100%, respectively. Considering this excellent flash DE, no correction factor has been applied to the data in the course of this study.

Even though EUCLID is an evolving network expanding gradually its boundaries and the amount and type of sensors participating over the years, it can be assumed that from 2004 onward the performance of the network has been optimal in the region of interest covering Belgium. A year-by-year analysis of the semi-major axis (SMA) of the 50% positional confidence ellipse and the average number of sensors used (ANSU) in the calculation of a solution reveals that SMA decreases from 400 m in 2004 to 100 m in 2013 with a median value of 300 m, while ANSU remains nearly stable around 13 throughout the period. Without going into too much detail, this gradual improvement over the years is attributed to sensor upgrades and the introduction of new techniques to process the raw data. Note that considering the fact that SMA is closely related to the actual LA (Diendorfer et al., 2014), the location accuracy improved accordingly. However, since in this work the details at scales of a few 100 meters are not considered, this will not influence the results of N_g presented further on. As regards to the DE, an improvement is expected to detect the individual strokes, but will hardly affect the flash DE. After all, in order to detect a flash it is sufficient to detect solely one out of several strokes in a multi-stroke flash.

Hence, we opt to use the CG flash data from 2004 to 2013 in this study within the domain

restricted to latitude 49° - 52° N and longitude 2° - 7° E as indicated by the dashed line in Fig. 1. The topography within this area is plotted as well, illustrating the difference in altitude between the west and east of Belgium. An increase in height toward the east/southeast is noticed up to a maximum elevation of 694 m.

3 Methodology

Initial stroke data are grouped into flashes based on a spatial and temporal clustering technique, with individual strokes belonging to a particular flash if $\Delta t \leq 1.5$ s and $\Delta r \leq 10$ km, with respect to the time and position of the first stroke in the flash. In addition, a temporal interstroke criterion, $\Delta t_{\text{interstroke}}$, of 0.5 s is used as well between subsequent strokes. These grouping criteria overlap well with those applied in other studies (e.g., Cummins et al. 1998; Kuk et al. 2011), except for the more relaxed time criterion, compared to a Δt of 1 s, which is traditionally used. Since occasionally flashes are observed with a duration exceeding 1 s (e.g., Poelman et al. 2013b), the time criterion used in this work is justified. The position of the first RS, being the center of the 50% positional confidence ellipse, is chosen as the position of the CG flash. Note that positive flashes with peak currents smaller than 10 kA are likely to be misclassified as CG flashes when in fact those are more likely to be of intracloud nature (Cummins et al. 1998; Wacker and Orville 1999a,b; Jerauld et al. 2005; Orville et al. 2002; Cummins et al. 2006; Biagi et al. 2007; Grant et al. 2012). Therefore, we opt to remove them from the dataset, decreasing the number of flashes by 4%.

Spatial distribution maps of flash density are obtained by summing the amount of flashes observed per grid cell and dividing it by the grids' area.

4 Results and analysis

4.1 Temporal statistics

Fig. 2a displays the temporal distribution of the CG flash counts for the years 2004-13 within the Belgian borders. As expected, the number of CG flashes experiences a natural variability over the years, with an observed minimum of about 14 000 flashes in 2010 and increasing up to a maximum of approximately 30 000 flashes in 2008. Typically, a thunderstorm season consists of several storm days. While thunderstorms appear in all shapes and sizes, the time scales at which these occur vary as well from short-lived events up to the more complex long-lived convective systems. Hence, only a handful of days typically contribute to the majority of the total number of CG flashes detected during an entire thunderstorm season. The observed annual variations are found as well in other parts of the globe, and are attributed to the natural variability of the climate (Ghil, 2002).

The distribution of the mean monthly flash count is shown in Fig. 2b. It is found that nearly 90% of the electrical activity occurs during May-August, with a peak in June-July. On the other hand, the winter months account only for one percent of the observed CG lightning activity in Belgium. This typical seasonal cycle is related to solar heating which peaks in summer and favours the onset of convective storms. In winter, thunderstorms are associated with the movement (passage) of cold fronts. In addition, the mean monthly amount of thunderstorm days in Belgium is plotted, with a thunderstorm day in this case being a day where any electrical activity has been observed regardless of its location within Belgium. It is found that the mean monthly amount of thunderstorm days varies between 4 and 16 days, and is in accordance with the values presented by Debontridder and Vandiepenbeeck (2008). By summing these monthly values, it follows that on average 104 stormdays occur per year in Belgium.

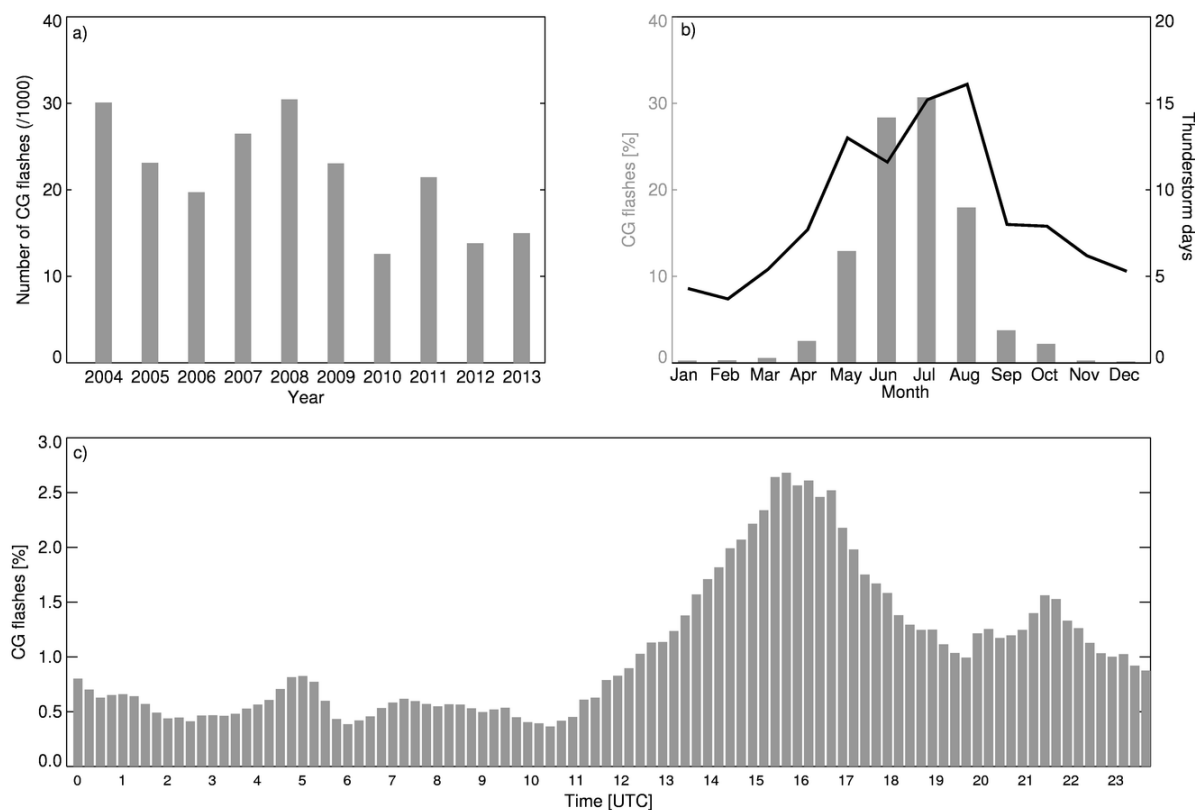


Figure 2: a) Annual cloud-to-ground flash counts, b) mean monthly cloud-to-ground flash counts expressed in percentage of the total activity (*grey*) and thunderstorm days (*black*), and c) mean diurnal flash counts (in %), based on 2004-13 EUCLID data.

In Fig. 2c the distribution of the diurnal flash count is indicated with a time resolution of 15 min and expressed in terms of percentage of the total CG flash activity. A minimum is observed during the morning hours, accompanied by a steady increase from 1100 UTC onward up to the maximum point in the afternoon at about 1500-1600 UTC. This is then followed by a decrease in activity until the morning hours, interrupted by a second moderate peak around 2100 UTC. Such a secondary moderate peak has been observed as well by Finke and Hauf (1996) in southern Germany and is believed to be caused by long-lasting storms propagating from their southwesterly source areas in easterly direction (Poelman et al. 2014). About 55% of the activity takes place between 1200 and 1900 UTC. Around 1100 UTC onward the activity rises as a result of solar heating of the ground, influencing the onset of convection. Nevertheless, a small peak is detected around 0500 UTC. An investigation into the cause of this peak reveals that it primarily stems from maximum one or two frontal thunderstorms per year. The overall diurnal behavior of CG flash counts overlap well with those in surrounding countries in Europe (e.g., Finke and Hauf 1996; Schulz et al. 2005; Antonescu and Burcea 2010; Mäkelä et al. 2014) or for instance in Brazil (Pinto et al. 1999b).

4.2 Spatial statistics

Knowing the total amount of CG flashes recorded within Belgium in between 2004-2013, it is easy to calculate the average flash density. It follows that $\langle N_g \rangle = 215\,000$ CG flashes / 30600 km^2 / 10 years = $0.7\text{ km}^{-2}\text{yr}^{-1}$.

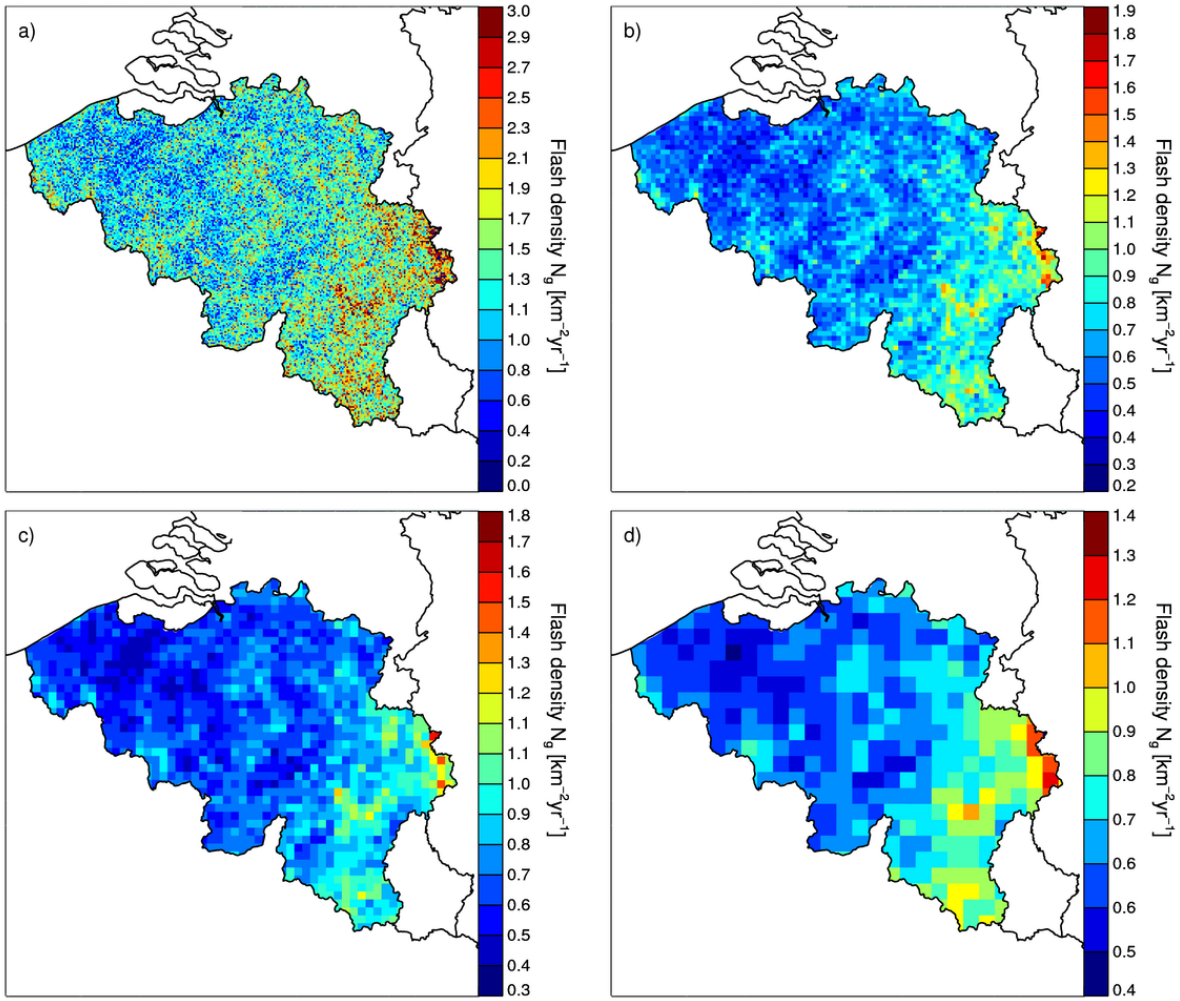


Figure 3: Spatial distribution of the mean annual flash density [$\text{km}^{-2}\text{yr}^{-1}$] adopting a spatial resolution of a) $1 \times 1 \text{ km}^2$, b) $3 \times 3 \text{ km}^2$, c) $5 \times 5 \text{ km}^2$, and d) $10 \times 10 \text{ km}^2$.

Fig. 3 plots the spatial variation of the mean annual flash density N_g [$\text{km}^{-2}\text{yr}^{-1}$] derived from 215 000 CG flashes adopting spatial resolutions ranging from $1 \times 1 \text{ km}^2$ to $10 \times 10 \text{ km}^2$. Obviously, lowering the grid resolution reduces the level of details present in the maps. In addition, it tends to influence the extent of the scale; reducing (/increasing) the maximum (/minimum) N_g value when the grid cell area is increased (/decreased). At first sight, it seems that the spatial distribution follows the orography, with the highest values found in elevated terrain. A quantitative analysis of this visual trend will be discussed later on.

At this point, the question arises what spatial grid is best suited to represent the lightning climatology in Belgium. There are two points of attention to be considered. First of all, it is essential that the grid size is larger than the assumed LA of the LLS. Since the relative LA of EUCLID is 600 m, a minimum grid resolution of 1 km^2 is therefore appropriate. Secondly, one could require to tolerate only a certain level of uncertainty of N_g . For this, it can be demonstrated that in order to obtain an uncertainty of less than 20% at 90% confidence level, a grid size has to be chosen in such a way that the dimensions of each cell and the number of years considered both comply with the minimum requirements by Eq. 2, following the Poisson distribution and the law of rare events (Diendorfer, 2008):

$$N_g \times T_{\text{obs}} \times A_{\text{cell}} \geq 80, \quad (2)$$

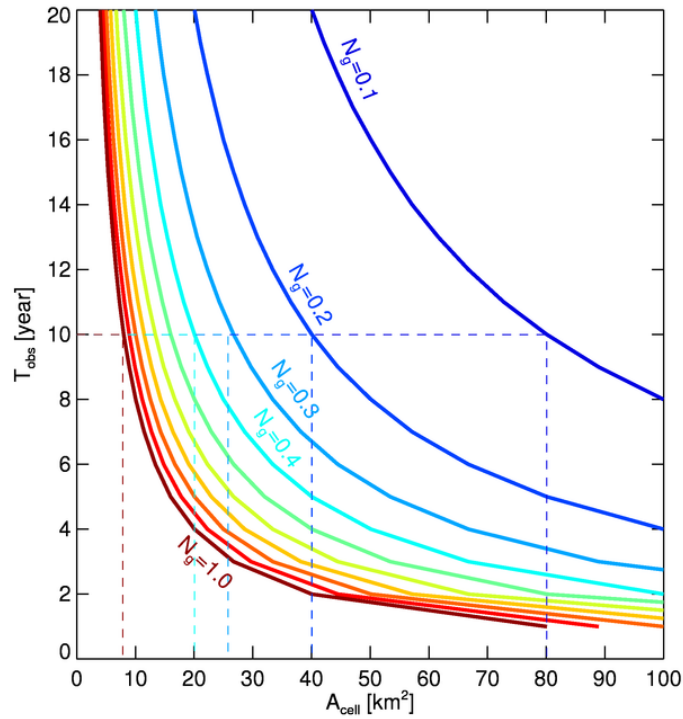


Figure 4: Minimum requirements as a function of number of years T_{obs} and grid cell area A_{cell} for different spatial flash densities N_g imposed by Eq. 2, in order to achieve an uncertainty of less than 20% at 90% confidence level.

with T_{obs} the observation period and A_{cell} the grid cell area expressed in years and km^2 , respectively. Thus, in a region of true value $N_g = 1$, about 80 events per cell could be achieved either by an observation period of 80 years with a 1 km^2 grid cell area or with a reduced observation period and an adequately increased grid size. The minimum requirements imposed by Eq. 2 are visualized in Fig. 4.

It is now straightforward to find out what spatial resolution is best suited applied to the data

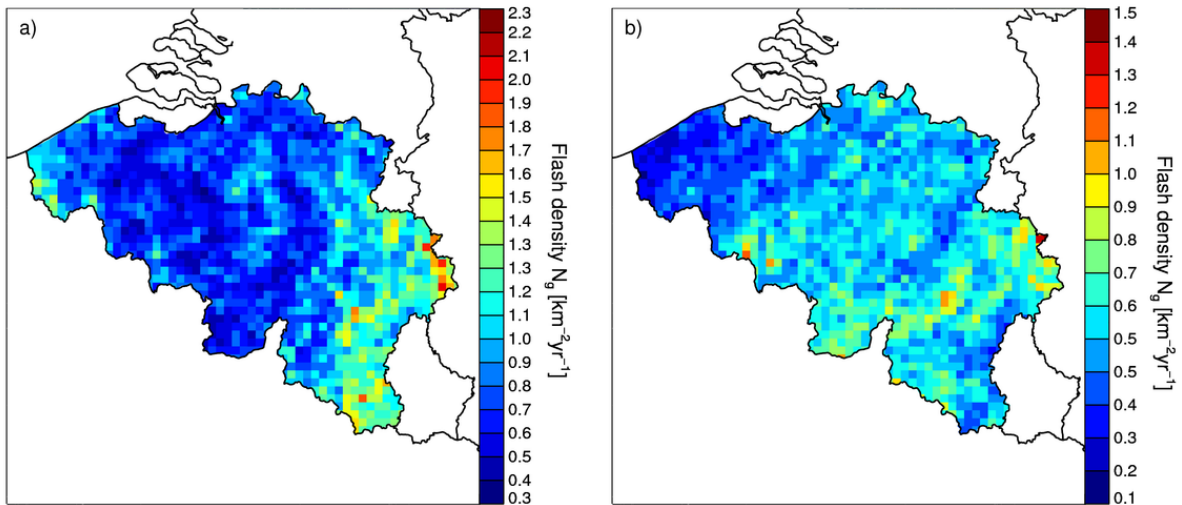


Figure 5: Spatial distribution of the mean annual flash density $[\text{km}^{-2}\text{yr}^{-1}]$ adopting a spatial resolution of $5 \times 5 \text{ km}^2$ for a) 2004-2008 and b) 2009-2013.

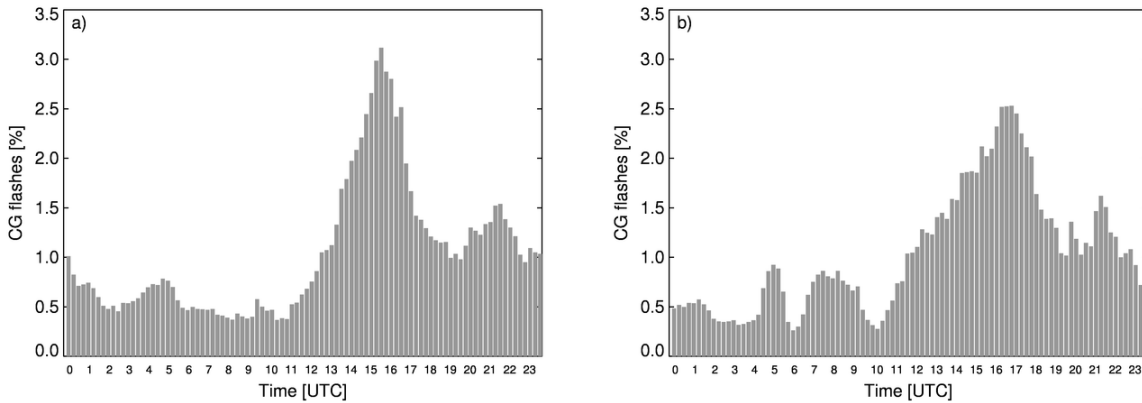


Figure 6: Mean diurnal flash counts, based on a) 2004-2008 and b) 2009-2013 EUCLID data.

set used in this study to present N_g in Belgium conform Eq. 2. For a fixed T_{obs} of 10 years, the required minimum grid cell area is indicated by the dashed lines for different N_g values. Using the average value of N_g of $0.7 \text{ km}^{-2}\text{yr}^{-1}$, it follows that Fig. 3c and 3d are conform Eq. 2. However, in order to maintain the highest level of detail possible, the $5 \times 5 \text{ km}^2$ spatial resolution is therefore the most appropriate choice to present the spatial distribution of the mean flash density in Belgium.

Note that, without any treatment of the data, N_g may differ by a few factors from one adjacent grid cell to another and is more apparent when the spatial grid area is small. One can speculate whether the observed small scale patterns reflect a climatological reality. It probably stems from the rather limited number of years used. However, since LLS evolve over time by upgrading their sensor technology and/or central processor software, one must be aware that a much larger data set has the disadvantage of entering discontinuities in the data. Either way, the end-user should be aware not to blindly trust the outcome of any LLS.

Fig. 5 splits the original data set into two sets of five years for the periods a) 2004–2008 and b) 2009–2014, in order to investigate whether the temporal and spatial behavior exhibits a similar trend compared to the full 10 year period. It is seen that the overall values in Fig. 5a are higher than in Fig. 5b. This is expected since the total amount of observed flashes is much larger during 2004-2008 than in 2009-2014, as evidenced from Fig. 2a. Even though the flash density differs to some extent between the two periods, the tendency of higher N_g towards the east/southeast of Belgium remains visible.

In a similar way, one can look at the effect on the distribution of the diurnal flash counts when applied on the two subsets, as shown in Fig. 6. Almost an identical diurnal behavior is observed compared to Fig. 2c, with a sharp increase of the electrical activity in the afternoon, followed by a decrease toward the evening. Note that there is a shift of about one hour in between the peaks of Fig. 6a and 6b.

The observed relation between N_g and topography as depicted in Fig. 3 and 5 has been studied by many authors in the past (Bourscheidt et al. 2007, Pinto et al. 1999). Such a relation is not surprising since variations in the surrounding terrain are known to influence the onset of convection and thus the development of thunderstorms (Orville 1965; Kottmeier et al. 2008; Hagen et al. 2011; Cummins 2014). This tendency is preserved for all the different grid resolutions in Fig. 3. To quantify the observed trend of higher flash densities at higher elevation, the mean flash density of CG flashes N_g as function of height and binning in 50 m altitude steps is plotted in Fig. 7. At sea level, the mean CG flash density is about $0.6 \text{ flashes km}^{-2}\text{yr}^{-1}$ and increases to approximately $1.2 \text{ flashes km}^{-2}\text{yr}^{-1}$ for heights between 550 and 600 m. The mean CG flash density for heights in between 600–650 m is not really representative due to the limited

amount of grid cells participating. The large variation in N_g per altitude results in major standard deviation values. Nevertheless, Fig. 7 displays some dependency between altitude and observed N_g , even for the limited range of altitudes present within Belgium. The same method can be applied onto the 5-year subsets. The correlation is strong for the 2004-08 subset, with the flash density increasing by a factor of ~ 2 between sea level and the maximum height in Belgium. This tendency is less pronounced when based on the 2009-13 data set, where the density increases by only 25% toward the highest point.

Parameterization functions are achieved after applying a simple linear regression onto the data points. This is displayed in Fig. 7. It is found that

$$N_g(H) = \begin{cases} 0.54 + (8.9 \times 10^{-4} \times H) & \text{for 2004-2013} \\ 0.59 + (1.3 \times 10^{-3} \times H) & \text{for 2004-2008} \\ 0.48 + (4.5 \times 10^{-4} \times H) & \text{for 2009-2013,} \end{cases} \quad (3)$$

with H the height in meters.

Based on the individual CG detections in the 10 year dataset, the related spatial distributions in terms of thunderstorm days T_d and hours T_h are plotted in Fig. 8. Here T_d and T_h can be considered as robust representations of the actual CG lightning density, since the observation of only one flash per day/hour is needed to increase T_d/T_h by one. Hence, it tends to normalize the temporal variations in flash DE that might be present in the data (Bourscheidt et al. 2012). Bourscheidt et al. (2012) conducted a comparison of T_d obtained through human observations and LLS data. They found that the least-biased agreement between the two datasets was found when selecting a radius of 8 km. Therefore, T_d and T_h presented in this study are obtained by

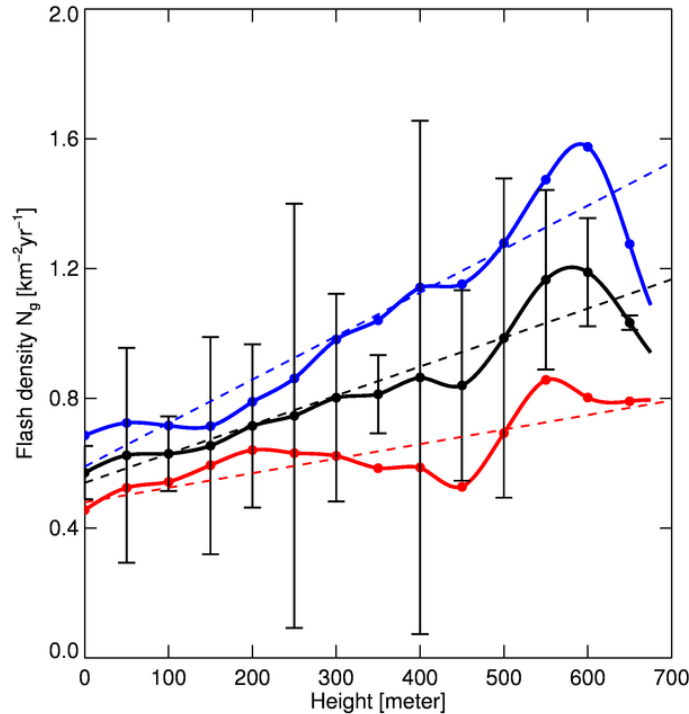


Figure 7: Distribution of the mean annual flash density [$\text{km}^{-2}\text{yr}^{-1}$] as a function of height in steps of 50 m in Belgium, based on 2004-13 EUCLID data (black). In addition, the ± 1 standard deviation is plotted as well. The distribution for the 2004-08 and 2009-13 subsets are displayed in blue and red, respectively. The respective parameterization functions are indicated as well (dashed lines).

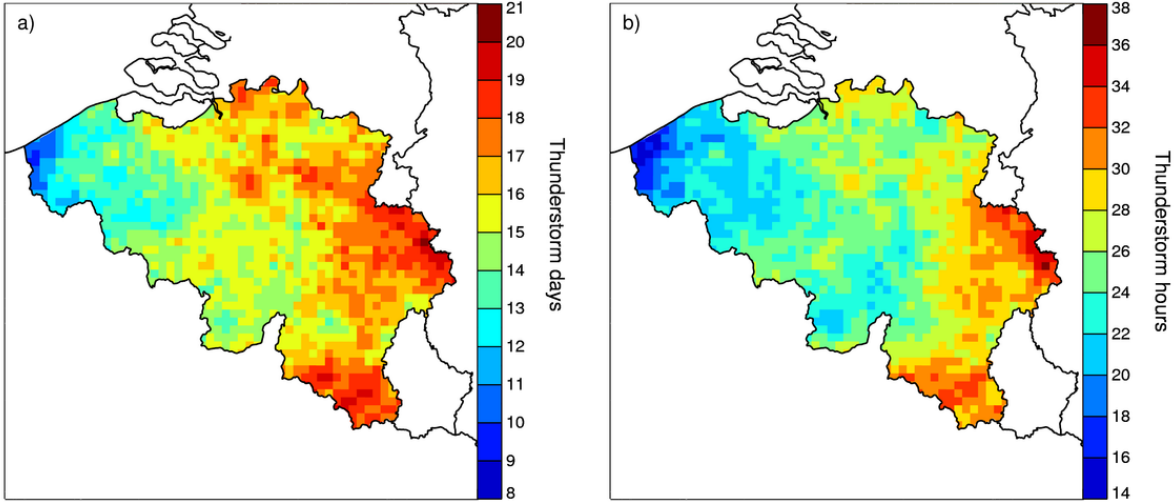


Figure 8: Spatial distribution of mean thunderstorm a) days and b) hours per year, based on 2004-13 EUCLID data and adopting a sound travel radius of 8 km and a spatial resolution of $5 \times 5 \text{ km}^2$.

looking in a radius of 8 km around each grid centroid whether lightning has been observed during a day and/or hour. If this is the case, the T_d and/or T_h increase by one. We find that T_d varies between 8 and 21 days in Belgium, with an average of 16 stormdays per year. The majority of thunderstorm days are located in the east and southeast of Belgium and drops off toward the west. Not surprisingly, the spatial pattern of T_d resembles the one found for N_g in Fig. 3. The same behavior is found for T_h , with values ranking between 14 and 38 h, with an average of 26 h of lightning activity averaged over 10 years. Note that with a larger (smaller) adopted sound travel radius T_d and T_h will increase (decrease) accordingly. Applying a similar regression as for N_g , it follows that

$$\begin{cases} T_d(H) = 15.05 + (5.18 \times 10^{-3} \times H) \\ T_h(H) = 23.89 + (1.43 \times 10^{-2} \times H), \end{cases} \quad (4)$$

with H the height in meters.

4.3 Presenting the data to the end-user

Electrically active storms come in different types and sizes. Typically, each year a handful long-lasting, giant storms dominate the charts in terms of number of CG flashes produced. These have a profound influence on the overall flash density in Belgium, while others, being short-lived and sporadic in nature, increase N_g within a limited area, with no impact what so ever a few kilometers further. Therefore, as pointed out earlier, a large variability in flash densities exists, with regularly a difference of a few factors in between adjacent grid cells. Whether this variability reflects the true climatological distribution of lightning flash densities in Belgium, or is a result of the size of the data set used, or is a combination of both, is complicated to determine.

Occasionally, the Royal Meteorological Institute of Belgium receives requests by, for instance, the media to provide the average flash density in a certain area of Belgium. Obviously, the answer can be presented in different ways and levels of detail. Nonetheless, in some cases a high level of detail is not a necessity. It could be more desirable to present the outcome by removing the smaller details but keeping the overall observed trend untouched.

In the following, we illustrate some of these possibilities which could be more accessible to the general public.

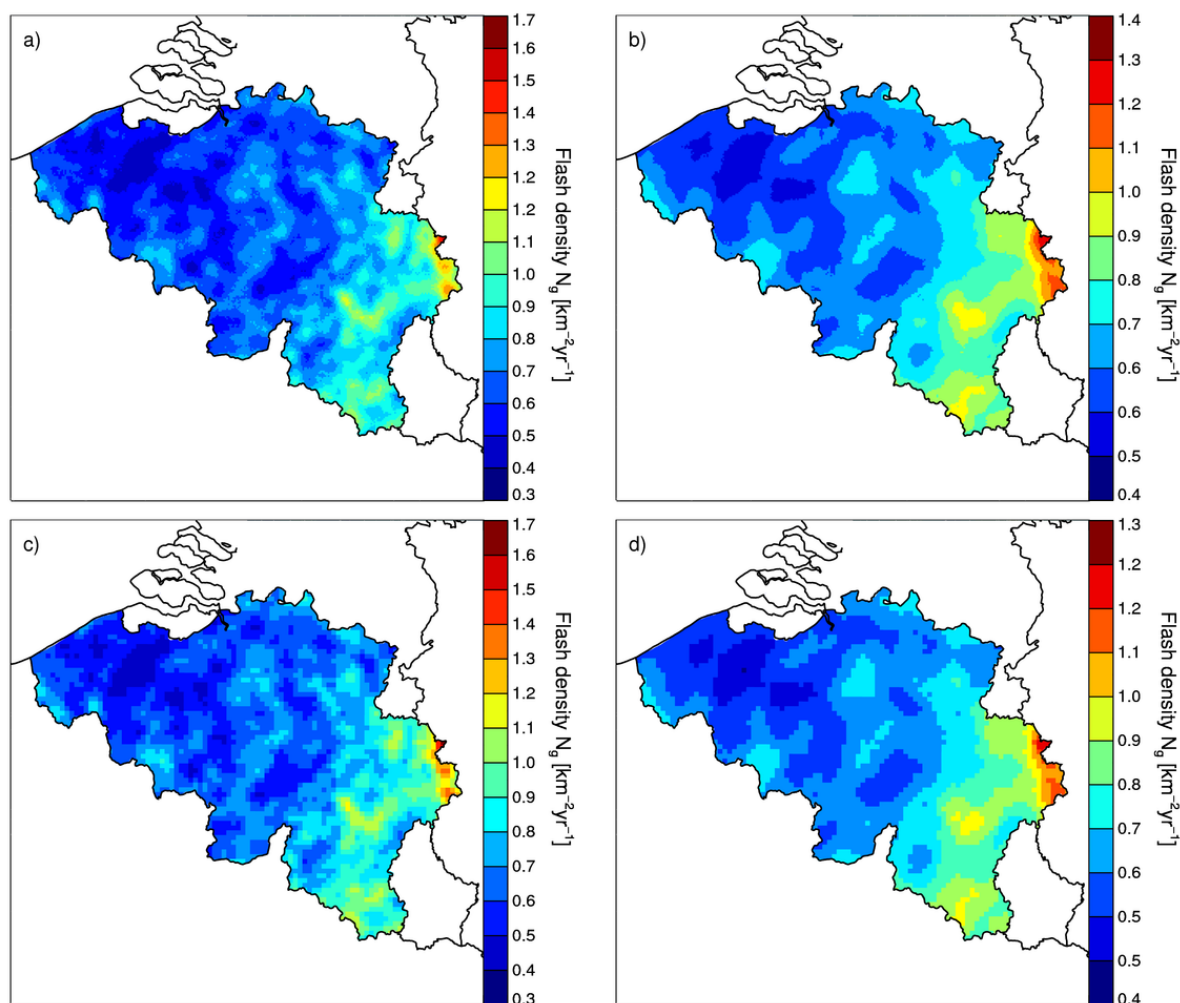


Figure 9: Spatial distribution of the mean annual flash density [$\text{km}^{-2}\text{yr}^{-1}$] adopting a spatial resolution of $1 \times 1 \text{ km}^2$, taking the mean value in a) 5 km radius and b) 10 km radius. c) and d) are similar to a) and b), but adopting a spatial resolution of $3 \times 3 \text{ km}^2$.

4.3.1 Smoothing

One way to account for this variability is by smoothing the data. For instance, one can calculate in each location of a grid the number of CG flashes recorded within a chosen radius and allocate the mean value within that circle as the flash density representative at this position. This is done in Fig. 9 for two different grid resolutions and radii.

One thing that strikes immediately is that for a fixed radius the level of detail is quasi equal among the different grid resolutions, as opposed to the N_g displayed in Fig. 3. On the other hand, the effect of a larger radius for a fixed spatial resolution is to lower (/increase) the maximum (/minimum) flash density observed in the grid cell and masks the finer details.

This simple method clearly is able to diminish the highly variable nature of N_g , while keeping the overall trend unaffected.

4.3.2 Lightning density at municipal and provincial level

Often the enquirer is only interested in a specific commune or province. Hence, in that case, it would be better to allocate a single value to a specific commune and/or province that best

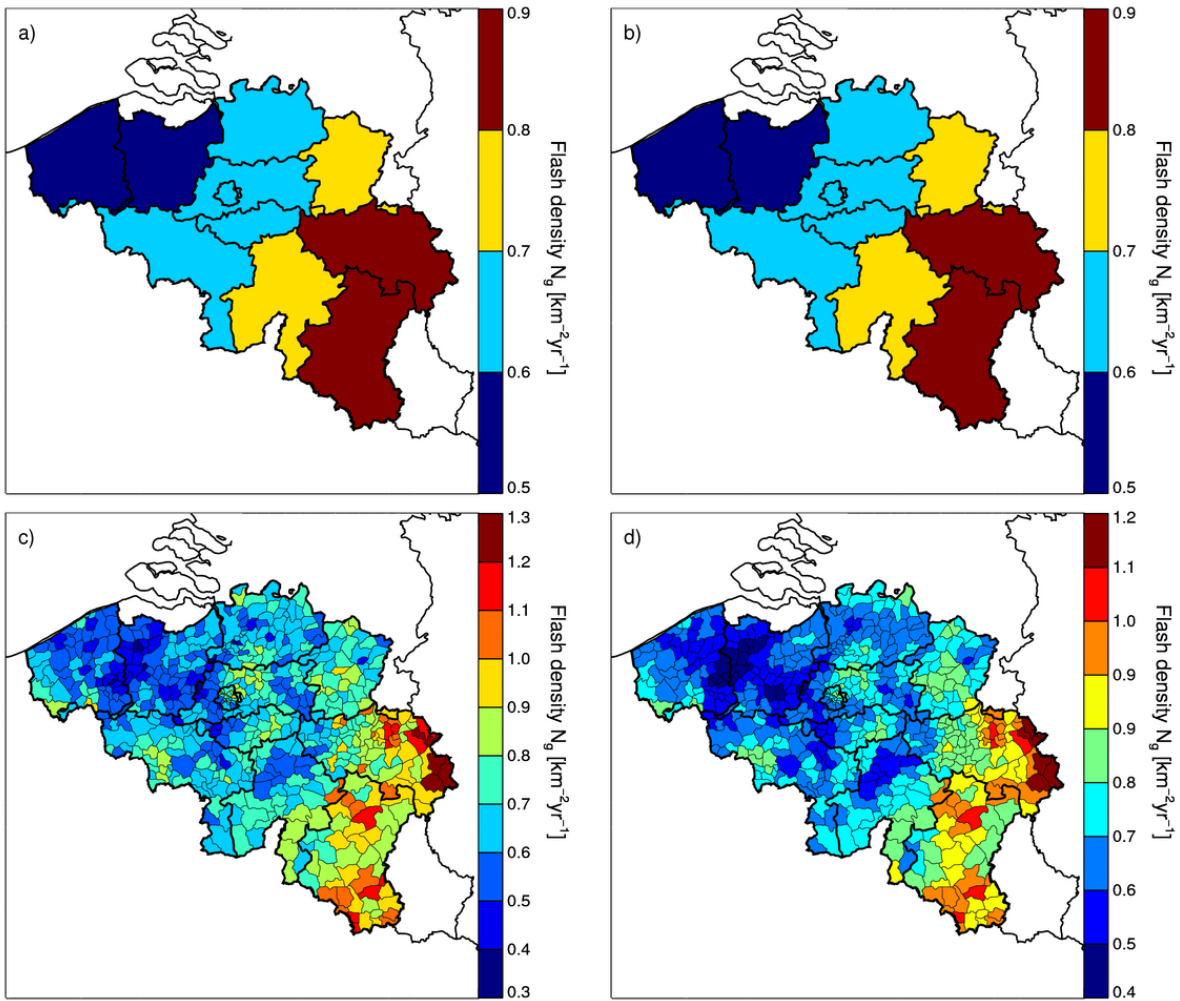


Figure 10: Flash densities [$\text{km}^{-2}\text{yr}^{-1}$] are plotted for each province (upper panels) and each commune (lower panels). The left panels appoint a value to each province/commune by summing the recorded flashes within the various borders and dividing it by the area of the respective province/commune. The right panels take the mean of the values of each 1 km^2 spatial grid points that fall within the borders, after smoothing within a 5 km radius.

represents the true value. This is done in Fig. 10. The left panels of Fig. 10 appoint a value to each province/commune by summing the recorded flashes within the various borders and dividing it by the area of the respective province/commune. The right panels of Fig. 10 take the mean of the values of each 1 km^2 spatial grid points that fall within the borders, after smoothing within a 5 km radius, analogue to Sect. 4.3.1.

On the level of the provinces, the outcome is identical. However, some differences are noticeable on the level of the communes. Typically, in Fig. 10c, the flash densities assigned to the smaller adjacent communes, can differ by a few factors. This is less so in Fig. 10d, where the change from one commune to the next is more gradual.

To highlight the latter, a zoom-in on Brussels and its communes is displayed in Fig. 11, analogue to Fig. 10c and 10d. One notices in Fig. 11a that within Brussels, a district with a moderate area of $\sim 160 \text{ km}^2$, communes differ in this way by almost a factor of 2. It either stems from very local effects such as high buildings attracting more lightning than the surrounding area. This in its turn increases the average lightning density, especially when the commune is small. Or, it could reflect the natural variability. The exact cause is hard to pinpoint and is out

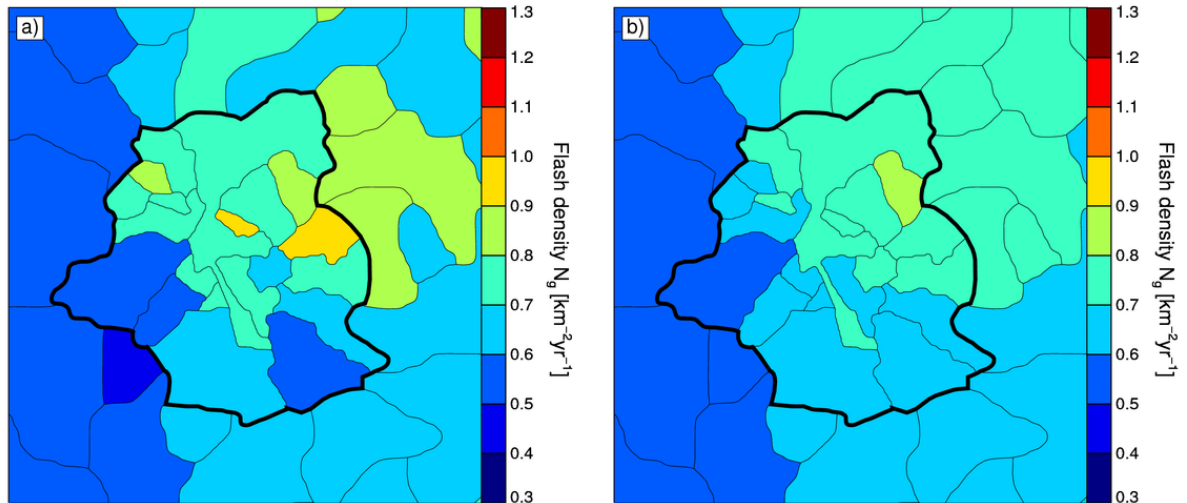


Figure 11: Analogue to Fig. 10, but zooming-in on Brussels, with a) the mean of the unaltered values of the underlying grid resolution of 1 km^2 and b) the mean of the smoothed values (5 km radius).

of the scope of this study. The latter variations mostly disappear when applying the smoothing algorithm within a radius of 5 km , before calculating the mean of the values that fall within the borders of the commune. In this way, local effects, if any, are smeared out and the lightning density in a certain commune agrees more closely with the surrounding communes.

5 Summary

Because of the variable nature of lightning occurrence from year to year, reliable insights into the lightning activity can only be achieved when based on large amounts of data. In this study, a total of 215 000 CG flashes recorded between 2004 and 2013 are used to analyze the temporal and spatial characteristics in Belgium.

It is found that the lightning activity primarily takes place during the summer months between May and August, accounting for about 90% of the total observed CG lightning activity in Belgium. The thunderstorm season reaches its peak in June-July. This is not surprising since solar heating of the ground, being one of the driving force of convective development, is most intense during this period. As regards the diurnal flash counts, those are the lowest during the morning hours, followed by a continuous increase from 1100 up to 1500-1600 UTC. Afterwards, a gradual drop brings the flash counts back to the observed level at dawn.

The topography of Belgium accounts for the spatial patterns observed in terms of flash density. For instance, flash density enhancements are visible toward the east and southeast of Belgium for regions above 300 m in comparison with the lower-lying areas toward the center and the coast. In addition, the geographical spread of T_d and T_h mirrors the behavior of N_g , since the computations are based upon the CG detections and an assumed sound travel radius. For the first time, the observed trend has been parameterized for N_g , T_d and T_h . The equations, as a function of height, can be used as a first approach to get an idea of the lightning characteristics corresponding to a particular region.

In addition, different graphical representations of N_g within Belgium are explored. This can be done in a more traditional way, allocating one value per grid cell for an adopted underlying spatial resolution. It is argued that, taking into account the moderate CG lightning intensity in Belgium, a $5 \times 5 \text{ km}^2$ spatial resolution is the most appropriate choice. One could also present the CG lightning density after applying a smoothing algorithm or assign one value to a particular

commune or province, whatever is closer to the preference of the enquirer.

Acknowledgments

The authors are grateful to the scientific committee for their helpful suggestions and advice on many aspects of this research.

References

- Antonescu, B., and S. Burcea, 2010: A cloud-to-ground lightning climatology for Romania. *Mon. Wea. Rev.*, **138**, 579-591, doi:10.1175/2009MWR2975.1.
- Biagi, C. J., K. L. Cummins, K. E. Kehoe, and E. P. Krider, 2007: National Lightning Detection Network (NLDN) performance in southern Arizona, Texas, and Oklahoma in 2003-2004. *J. Geophys. Res.*, **112**, D05208, doi:10.1029/2006JD007341.
- Bourscheidt, V., K. L. Cummins, O. Pinto Jr., and K. P. Naccarato, 2012: Methods to overcome lightning location system performance limitations on spatial and temporal analysis: Brazilian case. *J. Atmos. Oceanic Technol.*, **29**, 1304-1311, doi:10.1175/JTECH-D-11-00213.1.
- Cummins, K. L., 2014: Mapping the impact of terrain on lightning incidence and multiple ground contacts in cloud-to-ground flashes. *Proc. 15th Int. Conf. on Atmospheric Electricity*, Norman, OK, ICAE, 16 pp.
- , M. J. Murphy, E. A. Bardo, W. L. Hiscox, R. B. Pyle, and A. E. Pifer, 1998: A combined TOA/MDF technology upgrade of the U.S. National Lightning Detection Network. *J. Geophys. Res.*, **103**, 9035-9044, doi:10.1029/98JD00153.
- , J. A. Cramer, C. Biagi, E. P. Krider, J. Jerauld, M. A. Uman, and V. A. Rakov, 2006: The U.S. National Lightning Detection Network: Post-upgrade status. *Second. Conf. on Meteorological Applications of Lightning Data*, Atlanta, GA, Amer. Meteor. Soc., 6.1.
- Debontridder, L., and M. Vandiepenbeeck, 2008: Evolutie van het aantal onweersdagen in België. *Wetenschappelijke en technische publicatie*, **48**
- Diendorfer, G., 2002: EUCLID network performance and data analysis. *Proc. Int. Conf. on Grounding and Earthing and Brazilian Workshop on Atmospheric Electricity (GROUND/WAE)*
- , 2008: Some comments on the achievable accuracy of local ground flash density values. *Proc. 29th Int. Conf. on Lightning Protection*, Uppsala, Sweden, 6 pp.
- , H. Pichler, and W. Schulz, 2014: EUCLID located strokes to the Gaisberg Tower - accuracy of location and its assigned confidence ellipse. *Proc. Int. Lightning Detection Conf. and Int. Lightning Meteorology Conf. (ILDC/ILMC)*, Tucson, Arizona, USA
- , H. Zhou, and H. Pichler, 2011: Review of 10 years of lightning measurements at the Gaisberg tower in Austria. *Proc. Third Int. Symp. on Winter Lightning*, Sapporo, Japan, ISWL, 6 pp.
- Ducrocq, V., and Coauthors, 2013: HyMeX-SOP1: The field campaign dedicated to heavy precipitation and flash flooding in the northwestern Mediterranean. *Bull. Amer. Meteor. Soc.*, **95**, 1083-1100, doi:10.1175/BAMS-D-12-00244.1.
- Dwyer, J. R., M. Schaal, H. K., Rassoul, M. A. Uman, D. M. Jordan, and D. Hill, 2011: High-speed X-ray images of triggered lightning dart leaders. *J. Geophys. Res.*, **116**, D20208, doi:10.1029/2011JD015973.
- Finke, U., and T. Hauf, 1996: The characteristics of lightning occurrence in Southern Germany. *Beitr. Phys. Atmos.*, **69**(3), 361-374.
- Ghil, M., 2002: Natural climate variability. *Encyclopedia of Global Environmental Change. Volume 1: The Earth system: physical and chemical dimensions of global environmental change*, ISBN 0-471-97796-9
- Grant, M. D., K. J. Nixon, and I. R. Jandrell, 2012: Positive polarity: Missclassification between intracloud and cloud-to-ground discharges in the Southern African Lightning Detec-

- tion Network. *Proc. 22nd Int. Lightning Detection Conf.*, Broomfield, CO, Vaisala, 5 pp.
- Hagen, M., J. van Baelen, and E. Richard, 2011: Influence of the wind profile on the initiation of convection in mountainous terrain. *Quart. J. Roy. Meteor. Soc.*, **137**, 224-235, doi:10.1002/qj.784.
- Jerauld, J., V. A. Rakov, M. A. Uman, K. J. Rambo, D. M. Jordan, K. L. Cummins, and J. A. Cramer, 2005: An evaluation of the performance characteristics of the U.S. National Lightning Detection Network in Florida using rocket-triggered lightning. *J. Geophys. Res.*, **110**, D19106, doi:10.1029/2005JD005924.
- Kottmeier, C., and Coauthors, 2008: Mechanisms initiating deep convection over complex terrain during COPS. *Meteor. Z.*, **17**, 931-948, doi:10.1127/0941-2948/2008/0348.
- Mäkelä, A., S.-E. Enno, and J. Haapalainen, 2014: Nordic lightning information system: Thunderstorm climate of Northern Europe for the period 2002-2011. *Atmos. Res.*, **139**, 46-61, doi:10.1016/j.atmosres.2014.01.008.
- Orville, H. D., 1965: A photogrammetric study of the initiation of cumulus clouds over mountainous terrain. *J. Atmos. Sci.*, **22**, 700-709, doi:10.1175/1520-0469(1965)022.
- Orville, H. D., G. Huffines, W. Burrows, R. Holle, and K. Cummins, 2002: The North American Lightning Detection Network (NLDN) — First results: 1998-2000. *Mon. Wea. Rev.*, **130**, 2098-2108, doi:10.1175/1520-0493(2002)130.
- Pinto, I. R. C. A., O. Pinto Jr., R. M. L. Rocha, J. H. Diniz, A. M. Carvalho, and A. C. Filho, 1999b: Cloud-to-ground lightning in southeastern Brazil in 1993: 2. Time variations and flash characteristics. *J. Geophys. Res.*, **104**, 31 381-31 387, doi:10.1029/1999JD900799.
- Pinto, O., Jr., I. R. C. A. Pinto, M. A. S. S. Gomes, I. Vitorello, A. L., Padilha, J. H. Diniz, A. M. Carvalho, and A. C. Filho, 1999a: Cloud-to-ground lightning in southeastern Brazil in 1993: 1. Geographical distribution. *J. Geophys. Res.*, **104**, 31 369-31 379, doi:10.1029/1999JD900800.
- Poelman, D. R., F. Honoré, G. Anderson, and S. Pédeboy, 2013a: Comparing a regional, sub-continental, and long-range lightning location system over the Benelux and France. *J. Atmos. Oceanic Technol.*, **30**, 2394-2405, doi:10.1175/JTECH-D-12-00263.1.
- , W. Schulz, and C. Vergeiner, 2013b: Performance characteristics of distinct lightning detection networks covering Belgium. *J. Atmos. Oceanic Technol.*, **30**, 942-951, doi:10.1175/JTECH-D-12-00162.1.
- , 2014: A 10-year study on the characteristics of thunderstorms in Belgium based on cloud-to-ground lightning data. *Mon. Wea. Rev.*, **142**, 4839-4849.
- Prentice, S. A., 1977: Frequency of lightning discharges. *Lightning*, vol. I, Golde R. H., Academic Press, N.Y., pp. 465-496.
- Schulz, W., and G. Diendorfer, 2002: EUCLID network performance and data analysis. *Proc. Int. Lightning Detection Conference (ILDC)*, 5 pp.
- , K. Cummins, G. Diendorfer, and M. Dorninger, 2005: Cloud-to-ground lightning in Austria: A 10-year study using data from a lightning location system. *J. Geophys. Res.*, **110**, D09101, doi:10.1029/2004JD005332.
- , C. Vergeiner, H. Pichler, G. Diendorfer, and K. Cummins, 2012: Location accuracy evaluation of the Austrian lightning locations system ALDIS. *Proc. 22nd Int. Lightning Detection Conf.*, Broomfield, CO, Vaisala, 5 pp.
- , D. Poelman, S. Pédeboy, C. Vergeiner, H. Pichler, G. Diendorfer, and S. Pack, 2014: Perfor-

mance validation of the European Lightning Location System EUCLID. *Proc. Int. Colloquium on Lightning and Power Systems*, Lyon, France, CIGRE, 9 pp.

Wacker, R., and R. Orville, 1999a: Changes in measured lightning flash count and return stroke peak current after the 1994 U.S. National Lightning Detection Network upgrade: 1. Observations. *J. Geophys. Res.*, **104**, 2151-2157, doi:10.1029/1998JD200060.

—, and —, 1999b: Changes in measured lightning flash count and return stroke peak current after the 1994 U.S. National Lightning Detection Network upgrade: 2. Theory. *J. Geophys. Res.*, **104**, 2159-2162, doi:10.1029/1998JD200059.

A cloud-to-ground lightning climatology for Belgium
Dieter R. Poelman and Laurent Delobbe

Scientific committee:

Prof. dr. Ir. Christian Bouquegneau, dr. Maarten Reyniers,
dr. Christian Tricot, Luc Debontridder, dr. Michel Journée